Performance of RC Beams reinforced with Steel Fibers under Pure Torsion

Alan Mohammed Faidi Jehad
Department of Civil Engineering, College of Engineering, University of Baghdad, Iraq
A.Jehad1901m@coeng.uobaghdad.edu.iq (corresponding author)

Mohannad H. Al-Sherrawi
Department of Civil Engineering, College of Engineering, University of Baghdad, Iraq
Dr.Mohannad.Al-Sherrawi@coeng.uobaghdad.edu.iq

Received: 30 April 2024 | Revised: 11 May 2024 | Accepted: 13 May 2024

 DOI: https://doi.org/10.48084/etasr.7687

ABSTRACT

Reinforced Concrete (RC) beams are designed to resist torsion and shear and flexural failure due to applied loading. The failure mode of concrete elements owing to shear and torsion is unwanted and occurs without warning. So, in the design process it must be taken into account that if failure takes place, it is preferable for it to be flexural as this gives an indication before it occurs. The aim of the present study is to investigate the impact of using steel fibers with and without ordinary torsional reinforcements, on the torsional strength, crack distribution, and ductility of RC beams. The intended plan is to investigate the torsional capacity enhancement of RC beams with added steel fibers under monotonic torsional load. The finite element approach was adopted in the ABAQUS software in which the RC beams were simulated and the torsional load was applied. The results indicate that the presence of steel fibers within the concrete matrix raises torque resistance, reduces twist angle, and increases ductility, stiffness, and energy dissipation. An increase in the steel fiber percentage improves the performance of RC beam torque strength capacity and minimizes twist angle. The percentage of steel fiber has an important impact on the ultimate torque value. The ultimate torque increased by about 15, 21.6, 29, 39.3, 46.6, and 5.9% for 0.5, 1, 1.5, 2, 2.5 and 3%, respectively, added steel fibers, in comparison with the reference beam.

Keywords-stiffness; ductility; CFRP; reinforced concrete; flexural strength

I. INTRODUCTION

Reinforced Concrete (RC) beams under torsional moment have been investigated by many researchers with many different parameters taken into account. The international codes deal with the torsional moment effect on the RC beam with the equilibrium equations, which are functions of the mechanical properties of concrete and reinforcement to control this type of loading and prevent failure. The presence of Steel Fibers (SFs) has an impact on the strength and behavior of RC beams subjected to torsional moment. Percentage, aspect ratio, and type of SFs have influenced the results. The generated cracks in RC beams due to twisting are close, especially, near to the external supports and to the points of eccentric applied loads [1, 2]. The ultimate torque at failure increases as the compressive strength of the concrete increases [3] and decreases with T-girders with web openings under torsional loads, whereas the angle of twist increases [4]. The ultimate torsional resistance of the tested beams with pre-stressed strands increased by 73% [5].

SF concrete constitutes concrete containing short steel fibers within its matrix aiming to improve its mechanical properties [6]. The addition of SFs to concrete enhances its mechanical qualities, including its impact strength and tensile strength [7]. Bonding strength between SFs and concrete increases with increasing surface area between these two materials. Increasing the SF diameter, adding deformation in SF shape as anchorage or hooked ends, or increasing its aspect ratio do not always produce a stronger fiber connection due to the distribution of SFs and the workability of the SF mix [7]. Authors in [8] analyzed RC beams reinforced with SF subjected to pure torsion. The hollow cross section of RC beams was studied deploying the finite element method and ANSYS software. The torsional behavior SF RC specimens with low longitudinal reinforcement ratio subjected to pure torsion was experimentally investigated. A total of 10 specimens were tested and the recorded results, such as crack patterns, cracking torque, ultimate torsional strength, and torsional ductility by used ratio and type of SF were discussed. The results showed that the crack width of the end hooked SF specimens was wider than that of corrugated SF specimens, and decreased when the SF ratio increased with the end-hooked SF specimens exhibiting less cracks intensity. An increase in the percentage of SFs increases torsional resistance. Authors in [9] studied the contribution of hooked and straight SFs in enhancing the torsional and flexural resistance of RC beams. It was found that splitting tensile strength and compressive

strength increased when utilizing hooked SFs by 55.08 and 33.37%, respectively. In the presences of SF, the pre and post diagonal cracks were enhanced. There was no significant strain recorded in the main rebar's and flexural cracks were not developed. Large wide cracks in diagonal form, located at the middle-twisted region and near supports, were generated. All tested beams exhibited twisted mode of failure with the first crack occurring at the middle of the RC beams, while diagonal cracks appeared between the torque arms. Authors in [10] explored the torsional behavior and strength of Fiber RC Beams (FRCBs). The performance of FRCBs under applied torsion was investigated when the concrete matrix was mixed separately with polypropylene fibers (PPFs) and SFs. The results demonstrated that there was improvement in the torsional resistance and in the twist angle due to the presence of PPFs and SFs. The influence of SFs on the torsional beam resistance was greater than that of the PPFs. The authors recommended the use of 4% PPFs and SFs to enhance the behavior and strength of RC beams. Also, the presence of PPFs and SFs reduced crack width. The added SFs to the concrete matrix improved the torsional resistance and controlled the cracks. Authors in [11] studied the impact of SFs on the torsional strength of RC beams under pure torsion. The RC beams with dimensions of 300×300×2400 mm were reinforced only along the beam span without transverse reinforcements, whereas the concrete compressive strength was 25 and 50 MPa. The test results exhibited that for RC beams reinforced with SFs, after the cracks occurred, the torsional behavior was stable, the presences of SFs controlled the cracks and the torsional and cracked stiffness increased. It was reported that a low percentage of SF did not have a significant effect on the torsional resistance of the RC beams. Using SFs improved the initial and post cracks due to the applied torsional load. Authors in [12] estimated the minimum reinforcement to prevent torsional failure in the reinforced concrete and SF concrete members. The study aimed to suggest the minimum fiber factor as the minimum torsional reinforcement ratio. The results revealed that the presence of SFs with minimum torsional reinforcement improved the crack control.

II. AIM AND SIGNIFICANCE OF THE PRESENT STUDY

This paper presents the performance of RC beams reinforced with SFs with different percentages, i.e. 0.0, 0.5, 1.0, 1.5, 2.0, 2.5, and 3.0% under torsional load using the finite element approach in ABAQUS software. Some details that cannot be monitored in the experimental work, such as the interior crack proportions and the strain and stress in the compression and tension zone of concrete and reinforcement, are considered in the finite element analysis.

III. THEORETICAL ANALYSIS

Reinforced concrete beams, designed against torsional load and based on ACI-318-2019, according to a thin-walled tube space truss analogy were considered. The beams subjected to torsion were regarded as either perfect or better than in reality [6]. Cracking torque is calculated by:

$$T_{cr} = 0.33\lambda\sqrt{fc'}\ \left(\frac{A_{cp}^2}{P_{cp}}\right) \quad (1)$$

where λ is the modification factor (1 for normal concrete), A_{cp} is the enclosed area of the concrete beam, and P_{cp} is its outside perimeter. The nominal torsion of concrete member shall be less than the values given by:

$$T_n = \frac{2A_o\ A_t\ f_{yt}}{S}\ \cot\theta \quad (2)$$

$$T_n = \frac{2A_o\ A_l\ f_{yt}}{P_h}\ \tan\theta \quad (3)$$

where θ is the crack angle ($30 < \theta < 60$). The value of this angle can be taken as 45^o in the case of non-prestressed concrete member. A_t is the area of closed stirrups (one leg), A_l represents the longitudinal reinforcement area, and P_h is the center line perimeter of the closed stirrups (outer).

IV. MECHANICAL PROPERTIES OF CONCRETE, REINFORCEMENTS, AND STEEL FIBERS

The RC beam geometry and the mechanical properties adopted for concrete, reinforcements (main and stirrups), and SFs are listed in Tables I to V.

TABLE I. CONCRETE MECHANICAL PROPERTIES

Compressive strength f_c' (MPa)	Modulus of rupture (MPa)	Splitting tensile strength (MPa)	Modulus of elasticity (MPa)	Poisson's ratio
32	3.51	3.17	26587	0.2

TABLE II. CONCRETE BEAM GEOMETRY

Beam depth (mm)	Beam width (mm)	Cover (mm)		Main reinforcement		Stirrups diameter (mm)	Stirrups spacing (mm)
		Top	Bot.	Top	Bot.		
280	200	20	20	2Ø10	3Ø16	8	200

TABLE III. REINFORCEMENTS MECHANICAL PROPERTIES

Bar diameter (mm)	Reinforcement location	Tensile strength (MPa)	Modulus of elasticity (MPa)	Poisson' s ratio
16	Bottom longitudinal	532	200000	0.30
10	Top longitudinal	538	200000	0.30
8	Stirrups	567	200000	0.30

TABLE IV. STEEL FIBER GEOMETRY

Diameter (mm)	Length (mm)	Aspect ratio	Type
0.55	35	63.63	End-hooked

TABLE V. STEEL FIBER PROPERTIES

Ultimate strength (MPa)	Poisson's ratio
1345	0.3

V. CONCRETE MODEL

Concrete was modeled by Concrete Damage Plasticity (CDP) (plastic flow rule is Drucker-Prager yield surface) by defining five parameters to solve the Drucker-Prager plastic flow function and the yield function. These parameters are listed in Table VI.

TABLE VI. CONCRETE MODEL PARAMETERS

Dilation angle	Eccentricity ϵ	f_{b0}/f_{c0}	K_c	Viscosity
31	0.1	1.16	2/3	0.0001

To modify the shape of the plane meridians, plastic potential eccentricity ϵ representing the ratio of tensile to compressive strength was used. The angle of friction between concrete core and the surrounding steel tube was limited between 30 and 40°, so that the coefficient of friction was 0.6 for normal concrete for the adopted angle of friction (dilation angle) of 31°. The main and stirrup reinforcements were simulated to behave as full elastic. Von Mises yield criterion was utilized to determine the developed stress due to the applied torque in the reinforcements in the elastic limit to ensure its failure before concrete.

VI. COMPRESSIVE BEHAVIOR BY USING MENDER EQUATIONS

Mender unconfined stress strain curve was employed to represent the behavior of concrete by applying the below described equations.

- In case of $\varepsilon \leq 2\ \varepsilon_c'$ (curved portion), the stress is represented by:

$$f = \frac{fc'\ x\ r}{r-1+x^r} \quad (4)$$

where:

$$x = \frac{\varepsilon}{\varepsilon_c'} \quad (5)$$

$$r = \frac{E}{E-\frac{fc'}{\varepsilon_c'}} \quad (6)$$

- For $2\ \varepsilon_c' < \varepsilon \leq \varepsilon_u$ (linear portion) , the stress is represented by:

$$f = \left(\frac{2\ fc'\ r}{r-1+2^r}\right)\left(\frac{\varepsilon_u-\varepsilon}{\varepsilon_u-2\varepsilon_c'}\right) \quad (7)$$

where ε is the concrete strain, f is the concrete stress, E is the modulus of elasticity, fc' is the compressive strength of concrete, ε_c' is the strain of concrete at fc', and ε_u is the ultimate concrete strain capacity.

The tension behavior (stress-displacement) is found by the Hordijk equations:

$$f_{ct} = \sqrt{fc'}\ /\ 1.8 \quad (8)$$

$$\frac{\sigma(w)}{f_t} = [1+(c_1\frac{w}{w_{ult}})^3]\ e^{(-\frac{c_2 w}{w_{ult}})} - \frac{w}{w_{ult}}(1+c_1^3)\ e^{-c_2} \quad (9)$$

where w_{ult}=5.136×*Gf*/*ft*, c_1=3.00, c_2=6.93 and *Gf* and *ft* are parameters of the Hordijk model [14].

Figures 1 and 2 portray the stress-strain behavior of concrete in compression and tension, respectively. Figure 3 depicts the reinforcement stress-strain variation for the adopted yielding strengths.

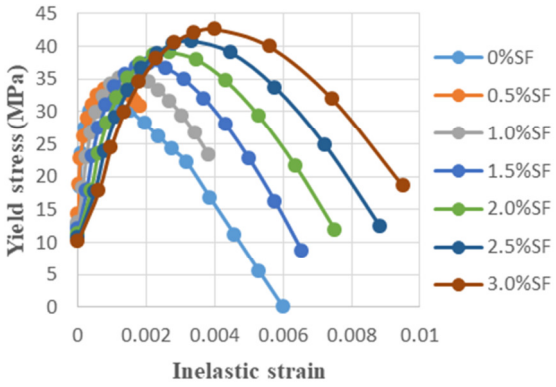

Fig. 1. Stress-strain of concrete with %SF in compression.

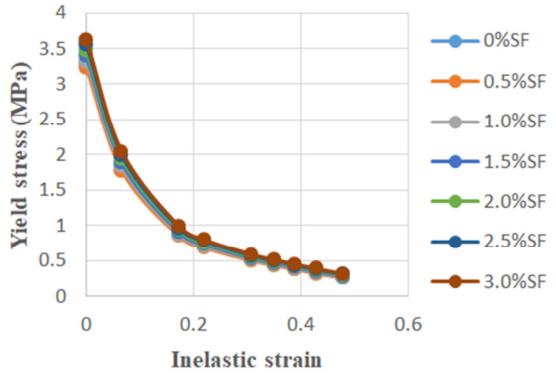

Fig. 2. Stress-strain of concrete with %SF in tension.

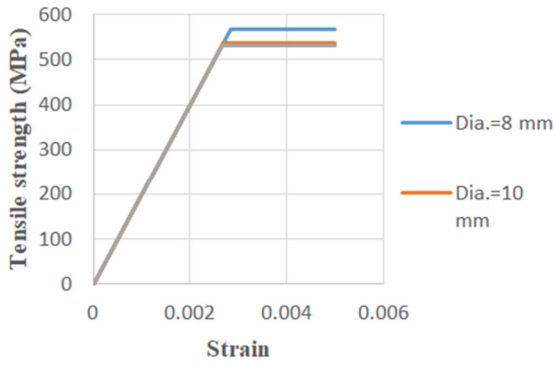

Fig. 3. Stress-strain of reinforcement.

VII. REINFORCED CONCRETE BEAM MODELS

RC beams were modeled under pure torsional load. The adopted RC beam design is evidenced in Figure 4. Table VII lists the models' descriptions which were analyzed using the finite element method in ABAQUS.

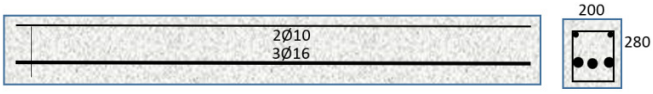

Fig. 4. RC beam details (all dimensions in mm).

TABLE VII. MODEL DESCRIPTIONS

Model Mark	B-0.0%	B-0.5%	B-1.0%	B-1.5%	B-2.0%	B-2.5%	B-3.0%
%SF	0.0	0.5	1.0	1.5	2.0	2.5	3.0

VIII. FINITE ELEMENT APPROACH

Three-dimensional finite element analysis was adopted to simulate the RC beams under pure torsion with and without the presences of SFs. The numerical analysis was based on the selected compatible with the problem mesh size and gave results with acceptable tolerance. The main assumptions when simulating the RC beams are:

- Plane section remains plane before and after the applied loading.
- There is full interaction between reinforcements and surrounding concrete, so that there is no shear friction at contact surfaces.
- Equivalent stress block diagram for the compression zone of reinforced concrete beams was used.
- The strain in the concrete and the reinforcement was proportional to their distance from the natural axis.
- The maximum strain (compressive) in concrete was limited to 0.003 based on [13].

Newton-Raphson numerical solution was utilized to reach a convergence solution by applied displacement control variable with accuracy 0.001. The adopted element types that model the RC beams giving performance similar to the actual behavior are eight-node brick elements for concrete and two-node truss elements for main and stirrups reinforcements. The presence of SFs within the concrete mix is calculated based on the analysis of the residual flexural stiffness of SFs and the new compressive strength is calculated according to the percentage of SF and then the tensile behavior of new concrete is determined. To simulate the concrete performance, second-order C3D8 tetrahedral elements were used. The C3D8 element has two important specifications as cracks and crush. The 2-node linear 3-D T3D2 truss element was put into service to simulate the main and stirrup reinforcement. The total number of nodes is 13900 and the total number of elements is 8736. The parts and mesh size of the RC beam in ABAQUS are illustrated in Figures 5 and 6.

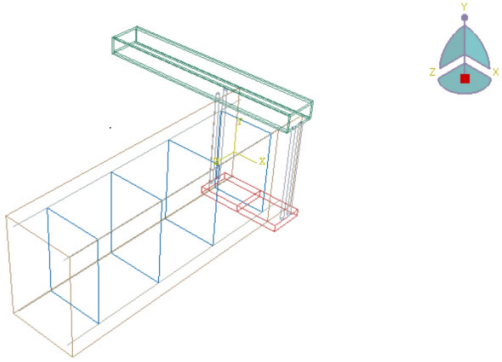

Fig. 5. Creating parts and assembly in ABAQUS.

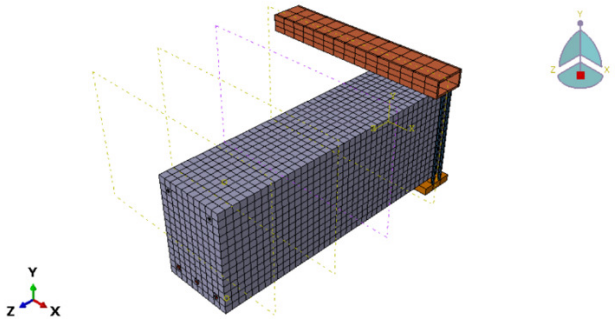

Fig. 6. RC with mesh arm to generate torque.

IX. STIFFNESS AND DUCTILITY

The torque-twist angle performance was calculated at the mid span for each point on the curve for all simulated models. The stiffness of the numerical analysis of the RC beams represents the resistance of an elastic body to deformation by an applied torque. The stiffness k_s is defined as the ratio of the ultimate torsional load T_u to the ultimate angle of twist $\emptyset_u$ as follows:

$$k_s = T_u / \emptyset_u \quad (10)$$

The stiffness of an RC concrete beam relies on the polar moment of inertia, the shear modulus, the beam span, and the applied torsional load. For the same beam geometry, the polar moment of inertia is constant, but the shear modulus differs according to the modulus of elasticity which depends on the concrete compressive strength (which depends on the percentage of SFs). The shear modulus plays an important role, so higher compressive strength gives higher shear modulus. Higher stiffness indicates that the RC beam has higher torsional carrying capacity with small twist angle due to the internal resistance of the RC beam.

The concrete ductility is the ability of the RC concrete beam to bear or endure considerable deformation prior failure. The ductility of the RC beam is very important because it provides indications regarding the quality and probable collapse or failure (an RC beam can undergo large deformations without failure). The concrete is a brittle material and the presence of SFs improves its mechanical properties. The ductility U of an RC beam is calculated by dividing the twist angle at failure torsional load $\emptyset_f$ by the twist angle at ultimate torsional load $\emptyset_u$:

$$U = \frac{\emptyset_f}{\emptyset_u} \quad (11)$$

X. ENERGY ABSORPTION OF RC BEAMS

The energy absorption is the area under the torsion-twist angle curve. The resistance of plain concrete against the applied torsional load is less due to the low energy dissipation and low resistance in tensile strength. The energy absorption can be adopted to evaluate the post-cracking behavior of the RC beams. The number of fibers in concrete affects this property of the RC beam in many ways (the presence of SFs improves the RC beam's post crack behavior). Increase in energy absorption reduces the effect of the applied torsional

load which spreads over a large area so that the produced pressure becomes less, thus producing less damage. The presence of SFs when the torsional load is applied has the ability to redistribute the applied torsional load and absorb it leading to increased energy absorption.

XI. ANALYSIS RESULTS

In this section, the finite element analysis results of torque-twist angle, stiffness, ductility, and energy dissipation of RC beams under torque load and concrete matrix reinforced by SF will be presented. The results are compared with those of the control beam (without SFs). Table VIII lists the maximum and failure torque and the corresponding twist angle of all models based on the considered SF percentages. Table IX exhibits stiffness, ductility, and energy dissipation of all models. Figure 7 shows the variations of the torque-twist angle of all models.

TABLE VIII. MAXIMUM AND FAILURE TORQUE AND CORRESPONDING TWIST ANGLE

Model mark	Maximum torque strength T_{max} (kN.m)	% Increase in T_{max}	Torque at failure (kN.m)	Twist angle at maximum torque ϕ (radian)	Twist angle at failure torque ϕ (radian)
B-0.0%	14.35	---	14.10	0.007523	0.008087
B-0.5%	16.51	15	16.48	0.02812	0.029713
B-1.0%	17.453	21.6	17.291	0.024578	0.034048
B-1.5%	18.52	29	16.08	0.03408	0.054064
B-2.0%	19.99	39.3	19.02	0.044877	0.063565
B-2.5%	21.03	46.6	20.89	0.0486	0.061533
B-3.0%	22.66	57.9	22.42	0.058884	0.073295

TABLE IX. STIFFNESS, DUCTILITY, AND ENERGY DISSIPATION

Model mark	Stiffness (kN.m/rad.)	Ductility	Energy dissipation (kN.m. rad.)
B-0.0%	1907.48	1.07	0.206
B-0.5%	587.13	1.06	0.941
B-1.0%	710.11	1.39	1.114
B-1.5%	543.43	1.59	2.153
B-2.0%	445.44	1.42	2.338
B-2.5%	398.14	1.27	2.391
B-3.0%	384.82	1.24	6.192

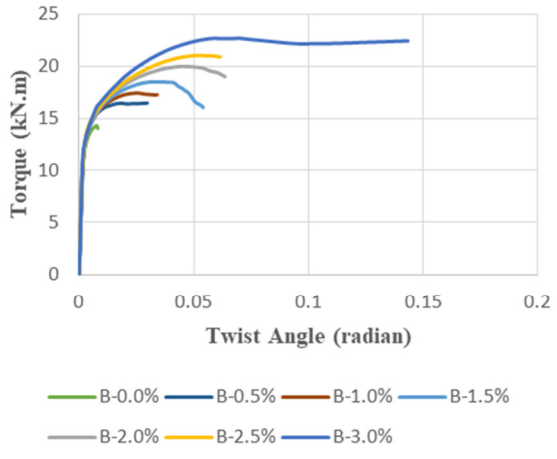

Fig. 7. Torque-twist angle variations for all models.

A. Torque-Twist Angle Performance

As seen in Figure 7, all models initially (up to the inflection point) behaved linearly. The inflection point differs from one model to another due to the differences in torque strength capacity. After the inflection point, the curve decreases up to failure due to the loss of resistance torque capacity and increased twist angle. Table X manifests the comparison between models' analysis results based on the SF percentage with the control model B-0.0% at maximum torque stage. Table X presents the values of the twist angle considered for each model due to the control torque of 14.35 kN.m.

TABLE X. TORQUE STRENGTH AND CORRESPONDING TWIST ANGLE

Model mark	Maximum torque strength (kN.m)	% Increase in torque capacity	Twist angle at maximum torque ϕ (radian)	% Decrease in twist angle
B-0.0%	14.35	---	0.007523	---
B-0.5%	16.51	15.05	0.004374	41.86
B-1.0%	17.45	21.60	0.004330	42.44
B-1.5%	18.52	29.06	0.003720	50.55
B-2.0%	19.99	39.30	0.003600	52.15
B-2.5%	21.03	46.55	0.003401	54.79
B-3.0%	22.66	57.91	0.002210	70.62

B. Ductility

Increased ductility means that the RC beam affords the deflection prior to failure, so this property is critical as it provides signs of failure and prevents total collapse. Table XI depicts the ductility values of all considered models.

TABLE XI. DUCTILITY OF ALL MODELS

Model mark	Ductility	% Increase
B-0.0%	1.07	---
B-0.5%	1.06	0.00
B-1.0%	1.39	29.91
B-1.5%	1.59	48.60
B-2.0%	1.42	32.71
B-2.5%	1.27	18.69
B-3.0%	1.24	15.89

C. Stiffness

Stiffness indicates the resistance to twist under the applied torque. An increase in stiffness means that the RC beam is more able to carry the applied torque with little twist angle. Increased SF percentages increase torque resistance due to the induced increase in torsional rigidity (increase in compressive strength). Table XII shows the comparison between the stiffness of the models with the control model.

TABLE XII. MODEL STIFFNESS

Model mark	Stiffness (kN.m/rad.)	Stiffness (kN.m/radian) with angle of twist as control	% Increase in stiffness
B-0.0%	1907.48	1907.48	---
B-0.5%	587.13	3280.75	71.99
B-1.0%	710.11	3314.09	73.74
B-1.5%	543.43	3857.53	102.23
B-2.0%	445.44	3986.11	108.97
B-2.5%	398.14	4219.35	121.20
B-3.0%	384.82	6493.21	240.41

D. Energy Dissipation

Energy dissipation represents the summation of the area of the torque-twist angle curve. The energy dissipation in RC beams attempts to take away the unwanted energy especially when subjected to seismic or wind loadings. Table XIII lists the energy dissipation values of all models. An increase in SF percentage increases the energy dissipation. Mixing SFs with concrete gives greater torque strength to the RC beam with less twist angle, so the energy dissipation of the beam increases.

TABLE XIII. ENERGY DISSIPATION

Model mark	Energy dissipation (kN.m. rad.)	Ratio of energy dissipation models to control model	% Increase in energy dissipation
B-0.0%	0.206	1.00	---
B-0.5%	0.941	4.57	356.80
B-1.0%	1.114	5.41	440.78
B-1.5%	2.153	10.45	945.15
B-2.0%	2.338	11.35	1034.95
B-2.5%	2.391	11.61	1060.68
B-3.0%	6.192	30.06	2905.83

XII. CONCLUSION

Based on the finite element analysis results, the presence of steel fibers within the concrete matrix increases the torque strength and reduces the twist angle. An increase in the steel fiber percentage leads to increased stiffness, ductility, and energy dissipation and overall improves the performance of reinforced steel fiber concrete beams under torque loading. The percentage of steel fiber has an important impact on the ultimate torque value. Increasing the percentage of steel fibers increased the ultimate torque by about 15, 21.6, 29, 39.3, 46.6, and 5.9% for the added steel fiber percentage of 0.5, 1, 1.5, 2, 2.5, and 3%, respectively, with respect to the reference beam.

The ductility of reinforced concrete beams in the presence of steel fibers is increased by the higher deformability of steel fibers whereas increasing the percentage of steel fibers (up to 2%) significantly improved ductility. The increase in the reinforced concrete beam twist angles indicates an increase in the ductility as compared with the control beam. Increased ductility means that the first occurrence of cracks is delayed. A linear performance was noticed in all considered models at the earlier stage of the applied torque up to the inflection point (first crack). Then, the twisting angle increased as the load increased.

REFERENCES

[1] S. K. Khalaf, A. A. Abdulhameed, and M. M. Kharnoob, "Behavior of Reinforced Concrete Continuous Beams Under Pure Torsion," *Journal of Engineering*, vol. 22, no. 12, pp. 1–15, Dec. 2016, https://doi.org/10.31026/j.eng.2016.12.01.

[2] A. J. Daraj and A. H. Al-Zuhairi, "The Combined Strengthening Effect of CFRP Wrapping and NSM CFRP Laminates on the Flexural Behavior of Post-Tensioning Concrete Girders Subjected to Partially Strand Damage," *Engineering, Technology & Applied Science Research*, vol. 12, no. 4, pp. 8856–8863, Aug. 2022, https://doi.org/10.48084/etasr.5008.

[3] A. A. H. Al-Nuaimi, R. M. Abbas, and R. B. Abbas, "Nonlinear Analysis on Torsional Strengthening of Rc Beams Using Cfrp Laminates," *Journal of Engineering*, vol. 19, no. 09, pp. 1102–1114, Sep. 2013, https://doi.org/10.31026/j.eng.2013.09.05.

[4] M. H. A.- Sherrawi and Z. M. Shanshal, "Torsional Resistance of Reinforced Concrete Girders with Web Openings," *Journal of Engineering*, vol. 22, no. 2, pp. 137–155, Feb. 2016, https://doi.org/10.31026/j.eng.2016.02.10.

[5] H. M. Husain, N. K. Oukaili, and M. M. Jomaa'h, "Effect of Prestressing Force Ontorsion Resistance of Concrete Beams," *Journal of Engineering*, vol. 13, no. 04, pp. 1902–1918, Dec. 2007, https://doi.org/10.31026/j.eng.2007.04.05.

[6] T. Błaszczyński and M. Przybylska-Fałek, "Steel Fibre Reinforced Concrete as a Structural Material," *Procedia Engineering*, vol. 122, pp. 282–289, Jan. 2015, https://doi.org/10.1016/j.proeng.2015.10.037.

[7] ACI Committee 544, *544.1R-96: Report on Fiber Reinforced Concrete (Reapproved 2009)*. Miami, FL, USA: ACI, 1996.

[8] J. K. Mures, A. H. Chkheiwer, and M. A. Ahmed, "Numerical Analysis of Hollow Cross Section Reinforced Concrete Beams Strengthened by Steel Fibers Under Pure Torsion," *Basrah journal for engineering science*, vol. 21, no. 3, pp. 50–54, Oct. 2021, https://doi.org/10.33971/bjes.21.3.6.

[9] M. Adnan Hadi and S. D. Mohammed, "Improving torsional – Flexural resistance of concrete beams reinforced by hooked and straight steel fibers," *Materials Today: Proceedings*, vol. 42, pp. 3072–3082, Jan. 2021, https://doi.org/10.1016/j.matpr.2020.12.1046.

[10] A. Karimipour, J. de Brito, M. Ghalehnovi, and O. Gencel, "Torsional behaviour of rectangular high-performance fibre-reinforced concrete beams," *Structures*, vol. 35, pp. 511–519, Jan. 2022, https://doi.org/10.1016/j.istruc.2021.11.037.

[11] L. Facconi, F. Minelli, G. Plizzari, and P. Ceresa, "Experimental Study on Steel Fiber Reinforced Concrete Beams in Pure Torsion," in *fib Symposium 2019*, Krakow, Poland, May 2019.

[12] H. Ju, S.-J. Han, D. Zhang, J. Kim, W. Wu, and K. S. Kim, "Estimation of Minimum Torsional Reinforcement of Reinforced Concrete and Steel Fiber-Reinforced Concrete Members," *Advances in Materials Science and Engineering*, vol. 2019, no. 1, 2019, Art. no. 4595363, https://doi.org/10.1155/2019/4595363.

[13] ACI 318-19, *ACI 318-19 Building Code Requirements for Structural Concrete*. Miami, FL, USA: ACI.

[14] D. Hordijk, *Local approach to fracture of concrete*. Delft, The Netherlands: Delft University of Technology, 1991.